Supporting Information

Fully 2D and 3D printed anisotropic mechanoluminescent objects and their application for energy harvesting in the dark

*Dinesh K. Patel, Bat-El Cohen, Lioz Etgar and Shlomo Magdassi**

S1. The rheology and mechanical properties of PDMS with varying concentration of platinum cure retarder.

As seen in Fig. S1 a, with increase in concentration of platinum cure retarder, the open time of the PDMS increases. Beyond 1% of platinum cure retarder, the open time increases drastically. The curing time is becomes very high (the viscosity doesn't change much with time) and printing resolution goes down as one printed layer slips above other. To have right balance between the open times for printing without hampering the resolutions of the printed layers, the concentration of platinum cure retarder was fixed to 1%.

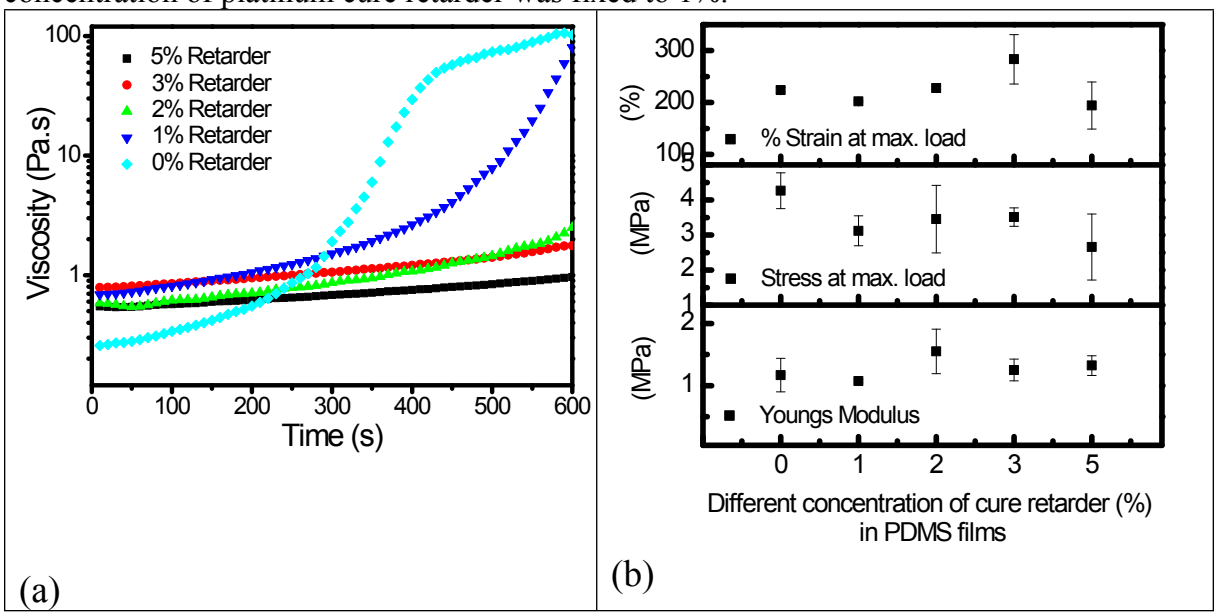

Figure S1. (a) The rheolgy and (b) mechanical properties of PDMS with varying concentration of platinum cure retarder (0-5%) to increase the open time of ink for 3D printing.

Mechanical properties of these films were also evaluated (Fig.S1 b). It was observed that the mechanical properties were improved until 2% of the retarder in PDMS. The films become tacky for higher percentage of retarder and curing time is high (Fig. S1a). To have right balance between curing time and mechanical properties, the concentration of retarder was fixed to 1% as stated above. Mechanical properties of ML films (PDMS and ZnS phosphor in ratio 3:7) with better performance were also evaluated as stated in earlier reports.[1-4] The young's modulus, elongation at break and stress at max. load was evaluated for ML films with PDMS and phosphor in ratio 3:7. The observed young's modulus, elongation at break and stress at max. load for these ML films were around 7.16± 1.47 MPa, 152.7± 38 % and 1.41± 0.14 MPa respectively.

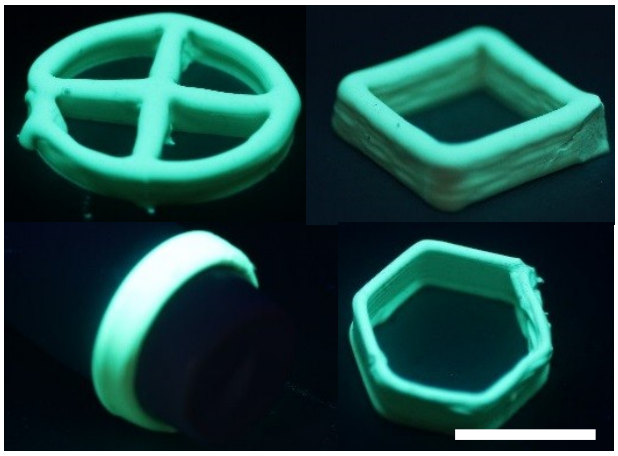

Figure S2. Images of luminescent ML devices under UV exposure at 365 nm. The scale bar is 10 mm.

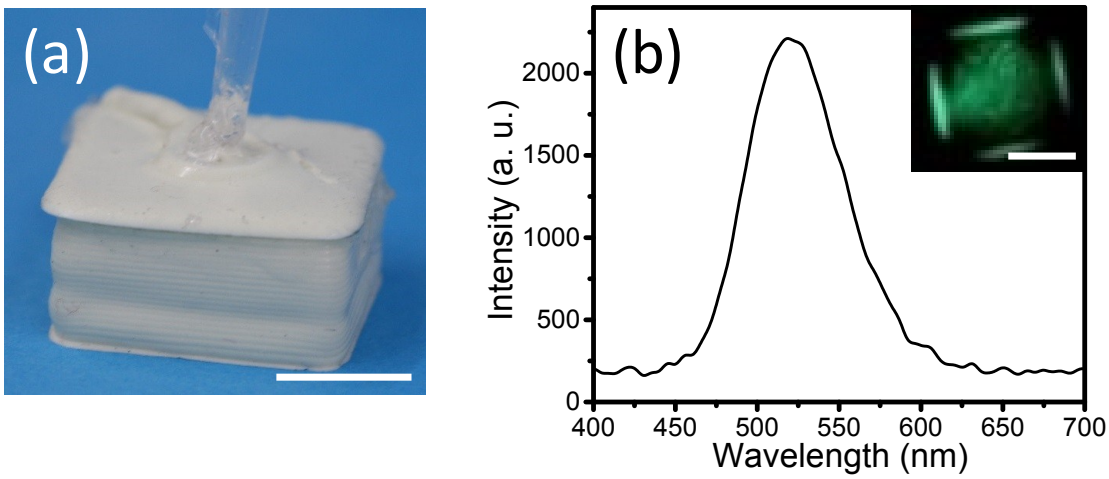

Figure S3. (a) 3D printed square balloon, (b) ML spectrum of a printed balloon (the inset shows a green ML balloon). The scale bar is 10 mm.

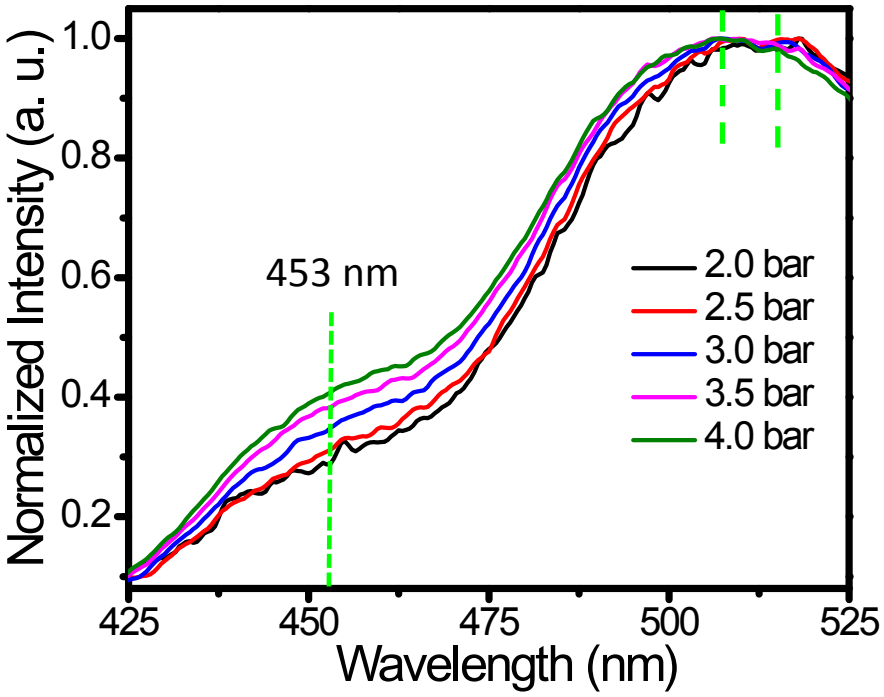

Figure S4. Normalized spectrum of a blue wind-driven ML device under nitrogen gas flow.

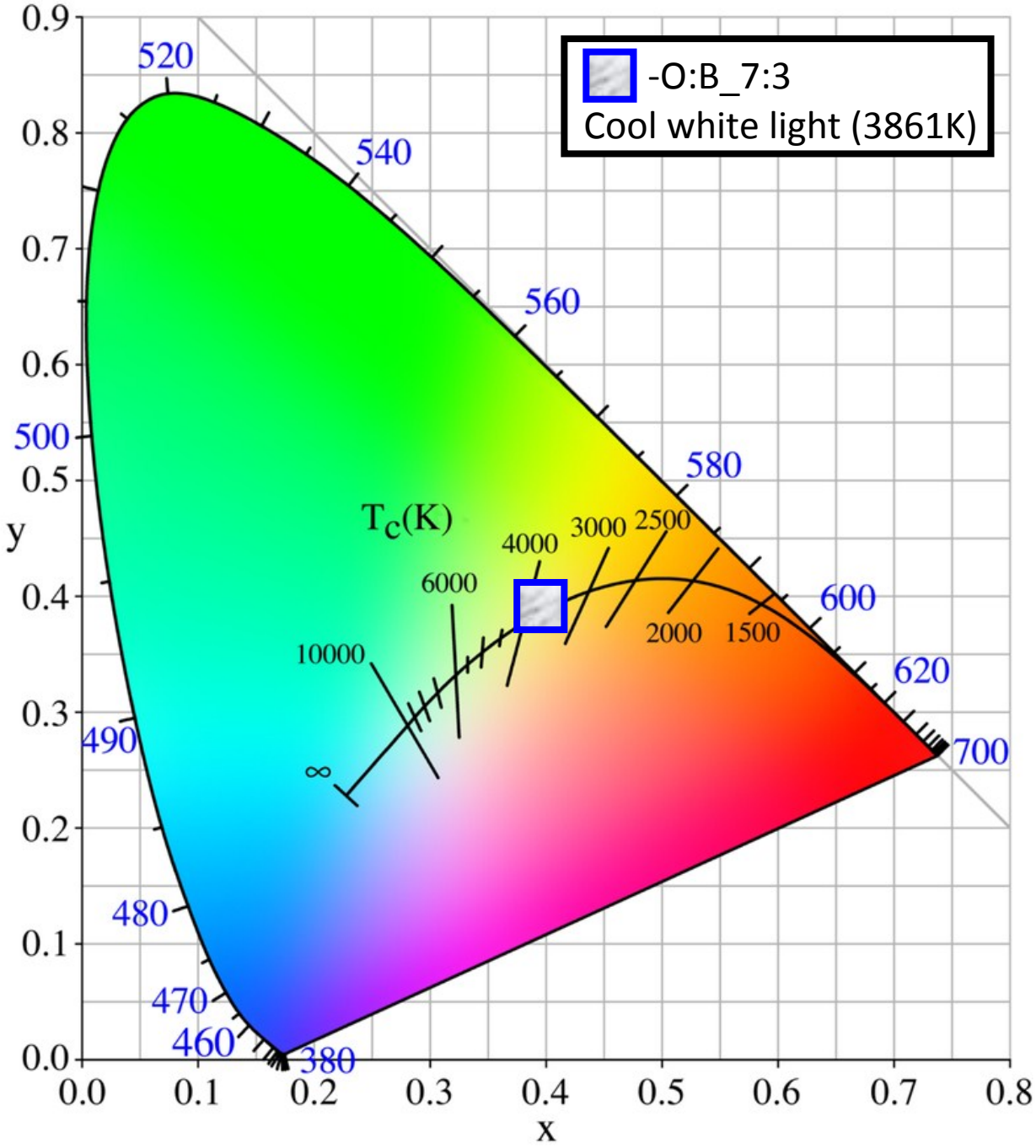

Figure S5. Cool white on CIE with a black body (Planckian) locus for a printed wind-driven ML device consisting of orange- and blue-emitting ZnS in a 7:3 ratio along with PDMS.

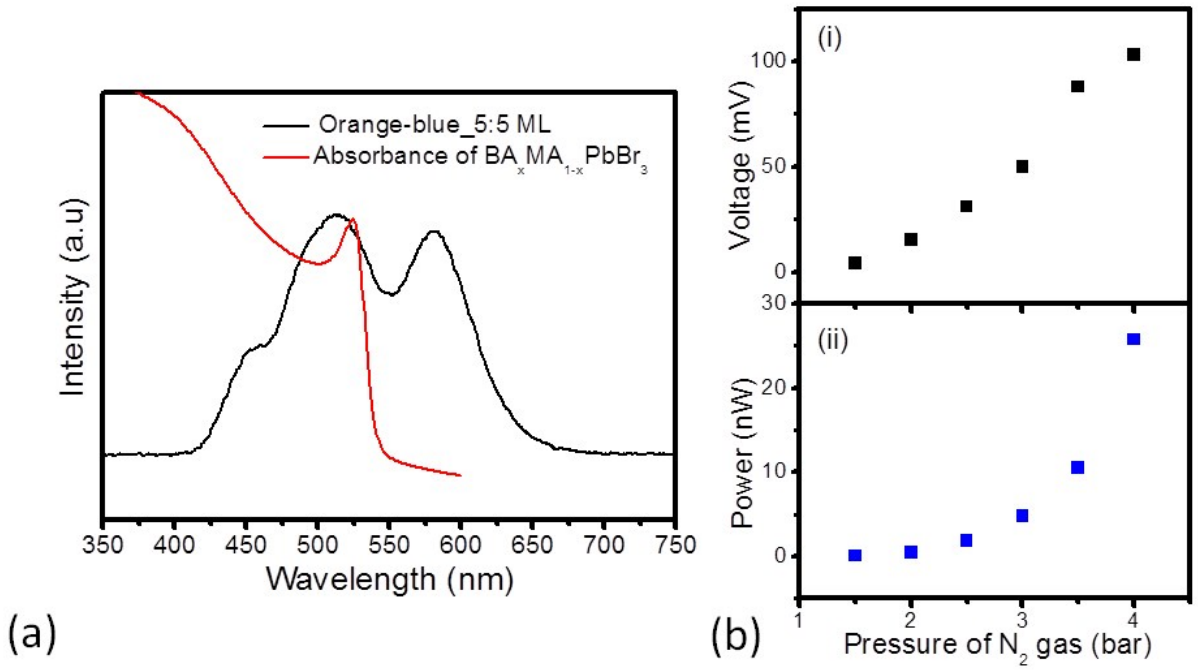

Figure S6 (a) Absorbance for a perovskite-based solar cell and ML emission from a wind-driven ML device with orange and blue phosphor in a 5:5 (weight %) ratio, (b) voltage and power generated by a wind-driven ML device coupled with a perovskite-based solar cell.

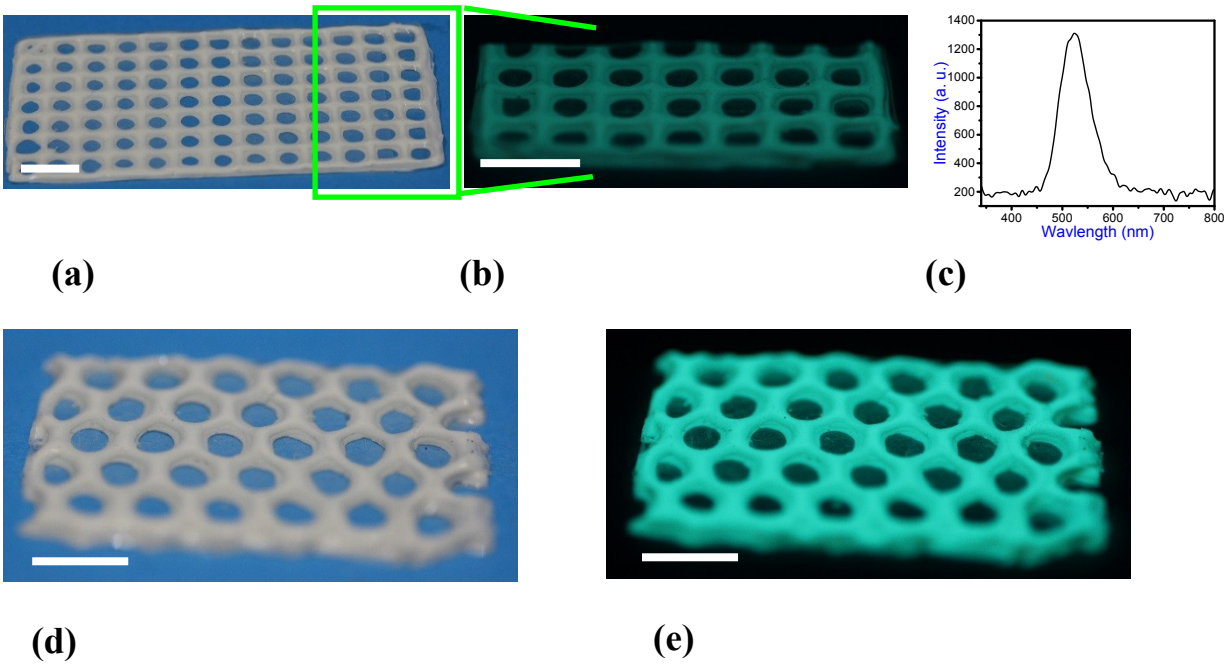

Figure S7. Fully printed patterned devices: (a, d) square and hexagonal meshes, (b, e) under UV (365 nm) irradiation, (c) ML spectrum from square mesh. The scale bar is 10 mm.

Movies

Movie S1	Video of 3D printed ML candy.
Movie S2	Video of a 3D ML balloon.
Movie S3	Fully printed wind-driven ML emitting green, orange, and blue.
Movie S4	Brightest wind-driven ML at 130 cd/m^2.
Movie S5	Patterned square mesh.
Movie S6	Dual-color-emitting hexagonal mesh.
Movie S7	Anisotropic mechanoluminescent (AML) device.

References

1 S. M. Jeong, S. Song, S.-K. Lee and B. Choi, *Appl. Phys. Lett.*, 2013, **102**, 051110.

2 S. M. Jeong, S. Song, S.-K. Lee and N. Y. Ha, *Adv. Mater.*, 2016, **25**, 6194–6200.

3 J. Zhang, L. Bao, H. Lou, J. Deng, A. Chen, Y. Hu, Z. Zhang, X. Sun, H. Peng *J. Mater. Chem. C,* 2017, **5(32)**, 8027-8032.

4 K.-S. Sohn, S. Timilsina, S. P. Singh, J.-W. Lee, J. S. Kim *ACS Appl. Mater. Interfaces* 2016, **8**, 34777−34783.